# Systematics of single and double $K$-shell-vacancy production in titanium bombarded by heavy ions

James Hall, Patrick Richard, Tom J. Gray, J. Newcomb, P. Pepmiller,* and C. D. Lin
*Department of Physics, Kansas State University, Manhattan, Kansas 66506*

K. Jones, B. Johnson, and D. Gregory*
*Brookhaven National Laboratory, Upton, New York 11973*
(Received 13 January 1983)

The systematics of single and double $K$-shell-vacancy production in titanium has been investigated in the limit of zero target thickness ($\sim 1$ $\mu$g/cm$^2$) for incident C, N, O, F, Mg, Al, Si, S, and Cl ions over a maximum energy range of 0.5 to 6.5 MeV/amu. This corresponds to collision systems with $0.27 \leq Z_1/Z_2 \leq 0.77$ and $0.24 \leq v_1/v_{2K} \leq 0.85$, where $v_1$ is the projectile nuclear velocity and $v_{2K}$ is the mean velocity of an electron in the target $K$ shell. The present work is divided into four major sections. (1) Single $K$-shell-vacancy production has been investigated by measuring $K\alpha$ and $K\beta$ satellite x-ray-production cross sections for projectiles incident with no $K$-shell vacancies. For incident ions with $Z_1 \geq 9$, the contribution due to electron-transfer processes from the target $K$ shell to outer shells of the projectile has also been noted. (2) Single $K$-shell—to—$K$-shell electron-transfer cross sections have been obtained indirectly by the measuring of the enhancement in the Ti $K$ x-ray production cross section for bare incident projectiles over ions incident with no initial $K$-shell vacancies. (3) Double $K$-vacancy production has been investigated by measuring the $K\alpha$ hypersatellite intensity in ratio to the total $K\alpha$ intensity. (4) Double $K$-shell—to—$K$-shell electron-transfer cross sections have been obtained indirectly with the use of a procedure similar to that used for single $K$ to $K$ transfer. The measured cross sections have been compared to theoretical models for direct Coulomb ionization and inner-shell electron transfer and have been used to investigate the relative importance of these mechanisms for $K$-vacancy production in heavy-ion—atom collisions.

## I. INTRODUCTION

Two of the principal mechanisms responsible for inner-shell vacancy production in ion-atom collisions are direct ionization and electron transfer. Until recently, the basic theoretical models for these processes have all been perturbative in nature and intended to be applicable to vacancy production by swift, point projectiles ($v_1/v_{2i} \gtrsim 0.1$ where $v_{2i}$ is the mean velocity of an electron in the $i$th target shell) interacting with more massive target atoms ($Z_1 \ll Z_2$). The classical impulse or binary-encounter approximation (BEA),[1] the impact-parameter-dependent semiclassical approximation (SCA),[2] and the quantum-mechanical plane-wave Born approximation[3] (PWBA) for direct ionization were all developed on this basis, as was the Oppenheimer, Brinkman and Kramers (OBK) approximation for electron transfer as formulated by Nikolaev.[4] Comparisons of these theories to ionization and electron-transfer cross sections for protons over a large range of target atomic numbers and incident ion energies[5] have demonstrated that the general trends of the experimental data for asymmetric collision systems are reasonably well predicted by these theoretical models. However, when heavier ions are used as projectiles, *ab initio* calculations for inner-shell vacancy production based on first-order perturbation theory generally prove to be inadequate. This has motivated extensive modifications to some existing theories and the development of new theoretical models for inner-shell vacancy production which go beyond first-order perturbation theory.[6–9]

In the present work, we extend the investigation of $K$-vacancy production in heavy near-symmetric collision systems ($Z_1 \lesssim Z_2$) focusing on the ionization and electron transfer channels at low to intermediate collision velocities ($v_1 \lesssim v_{2K}$). We provide a broad range of self-consistent data free of ambiguities due to target thickness effects[10] for comparison to current theoretical models for ionization and electron transfer. The projectile energy, atomic number, and charge-state dependence of $K$-vacancy production in Ti bombarded by heavy ions are studied near the limit of zero target thickness ($\sim 1$ $\mu$g/cm$^2$) for incident C, N, O, F, Mg, Al, Si, S, and Cl ions over a maximum energy range of 0.5 to 6.5 MeV/amu. This corresponds to collision systems with $0.27 \leq Z_1/Z_2 \leq 0.77$ and $0.24 \leq v_1/v_{2K} \leq 0.85$. Additional data for H,[11] He,[12,13] Li,[14] and B (Ref. 15) are taken from the literature to extend the study to collision systems with $Z_1/Z_2$ as low as $\sim 0.05$. Figure 1 shows the complete range of collision systems to be studied in terms of relative atomic numbers and scaled projectile velocities.

The present work is divided into four major sections. (1) Single $K$-vacancy production is investigated by measuring $K\alpha$ and $K\beta$ satellite x-ray-production cross sections for projectiles incident with no $K$-shell vacancies ($\sigma_{KX}^0$). For incident ions with $Z_1 \geq 9$, the contribution due to electron-transfer processes from the target $K$ shell to outer shells of the projectile is noted. (2) Single $K$-shell—to—$K$-shell electron-transfer cross sections are obtained indirectly by measuring the enhancement in the Ti $K$ x-ray-production cross section for bare incident projectiles ($\sigma_{KX}^2$) over ions incident with no initial $K$-shell vacancies ($\sigma_{KX}^0$), i.e., $\sigma_{KX}^{K\text{-}K} = \sigma_{KX}^2 - \sigma_{KX}^0$. (3) Double $K$-vacancy production

 

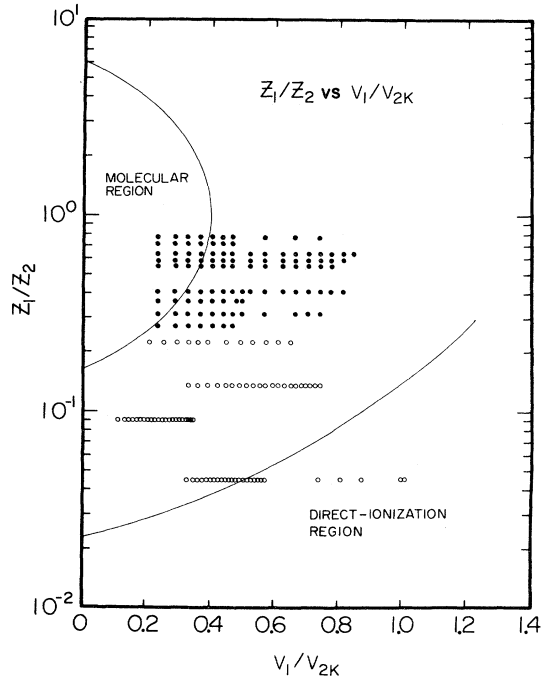


FIG. 1. Systematic plot of $Z_1/Z_2$ vs $v_1/v_{2K}$ for various projectiles incident on Ti $K$ shell. Filled circles represent data taken in this work and open circles represent data taken from the literature. The labeled regions indicate the approximate regions of validity for molecular orbital calculations and early (Refs. 1–3) direct-ionization calculations.

is investigated by measuring the $K\alpha$ hypersatellite x-ray intensity ratio to the total $K\alpha$ x-ray intensity. $K\alpha$ hypersatellites are x rays originating from states with double $K$-shell vacancies. (4) Double $K$-shell—to—$K$-shell electron-transfer cross sections are obtained indirectly by measuring enhancements in Ti $K\alpha$ satellite and hypersatellite intensities for projectiles incident with and without initial $K$-shell vacancies. Measured ionization cross sections are compared with calculations by Basbas, Brandt, and Laubert[6,7] which include as corrections to the PWBA the effects of Coulomb deflection of the projectile in the field of the target nucleus, increased binding energy of the target electrons due to the presence of the projectile, and high-velocity polarization of the target electron density. Electron-transfer cross sections are compared with recent coupled-state calculations by Lin *et al.*[8] and Reading, Ford, and Becker.[9] Preliminary results from this work have been reported in two previous publications.[16,17]

## II. EXPERIMENT

The experiment was performed using beams of C, N, O, F, S, and Cl, in the 0.50 to 2.25 MeV/amu range obtained from the model-*EN* tandem Van de Graaff accelerator at the James R. Macdonald Laboratory, Kansas State University along with beams of N, F, Mg, Al, Si, and Cl in the 2.0 to 6.5 MeV/amu range obtained from the model-*MP* tandem Van de Graaff accelerator at Brookhaven National Laboratory. These beams were obtained in charge states corresponding to zero, one, and two initial $K$-shell vacancies and were then focused onto thin ($\sim 1\ \mu g/cm^2$) transmission-mounted Ti foil targets oriented 45° with respect to the beam axis. Thin targets were used in order to approach single-collision conditions and thus avoid ambiguities in x-ray yield measurements due to target thickness effects.[10] Titanium $K$ x rays were detected by a solid-state Si(Li) detector (resolution $\sim 175$ eV at 5.9 keV) mounted in vacuum at a laboratory angle of 90° with respect to the beam axis. Simultaneously with x-ray detection, projectile ions scattered by a thin layer of Au ($\sim 5\ \mu g/cm^2$) evaporated onto the back side of each target were detected by a surface barrier detector mounted in vacuum at a laboratory angle of 30°. Assuming Rutherford scattering of the incident ions, the effective target $K$ x-ray-production cross section for a given projectile atomic number, energy, and incident charge state can be related to the yield of target $K$ x rays per scattered ion by

$$\sigma_{KX}=k(Z_1/E_1)^2(Y_{KX}/Y_P)\ ,$$

where the constant of proportionality $k$ may be determined by normalizing to a previous measurement. The cross sections determined in this work were normalized to a measured value of $\sigma_{KX}=(6.63\pm 0.99)\times 10^{-21}$ cm$^2$ for 1.7 MeV/amu $F^{5+}$ + Ti due to Schmiedekamp *et al.*[18]

The relative error associated with the data was dominated by a reproducibility error in $(Y_{KX}/Y_P)$ of $\sim 15\%$. Adding this in quadrature to a normalization error of $\sim 15\%$ gives an absolute error in $\sigma_{KX}$ of $\sim 20\%$.

## III. ANALYSIS

### A. Cross sections

The energy resolution of the detector was sufficient to distinguish the hypersatellite x rays due to the decay of double $K$-vacancy states from the satellite x rays due to the decay of single $K$-vacancy states. A least-squares analysis of the low-resolution Ti x-ray spectra thus allows the total x-ray-production cross section $\sigma_{KX}$ to be separated into satellite and hypersatellite components as shown in Fig. 2. The cross section for hypersatellite production, $\sigma_{KX}(H)$, is obtained from a ratio of x-ray yields according to $\sigma_{KX}(H)=\sigma_{KX}(Y_{K\alpha^h}/Y_{K\alpha^{\text{total}}})$ and is related to the double $K$-vacancy-production cross section, $\sigma_{\text{DKV}}$, by $\sigma_{KX}(H)=\omega_K\sigma_{\text{DKV}}$. The satellite component, corrected for cascade from double $K$-vacancy states, is given by $\sigma_{KX}(S)=\sigma_{KX}-2\sigma_{KX}(H)=\omega_K\sigma_{\text{SKV}}$, where $\sigma_{\text{SKV}}$ is the single $K$-vacancy-production cross section and where we have assumed that the hypersatellite fluorescence yield is equal to the average $K$-shell fluorescence yield $\omega_K$.

The relative error in experimental values of $\sigma_{KX}(S)$ is $\sim 15\%$, i.e., on the order of the relative error in $\sigma_{KX}$. Subtracting the hypersatellite yield has only a small effect on the relative error in $\sigma_{KX}(S)$ due to the relative magnitudes of the two cross sections. The absolute error in $\sigma_{KX}(S)$ is $\sim 20\%$. The relative error in experimental values of $\sigma_{KX}(H)$ is $\sim(20\text{–}25)\%$. The absolute error in $\sigma_{KX}(H)$ is $\sim(25\text{–}30)\%$.

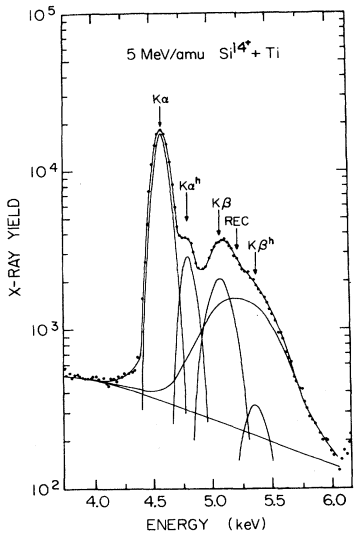


FIG. 2. Ti $K$ x-ray spectrum observed in low resolution for 5 MeV/amu $Si^{14+}$ + Ti. The principal features of the x-ray energy spectrum, as stripped out by least-squares analysis, are shown beneath the data. The broad structure labeled REC (radiative electron capture) is a kinematic peak associated with the capture of a loosely bound target electron directly into an inner shell of the projectile. The $K$-shell REC peak moves through the Ti $K$ x-ray lines as the projectile energy is increased from 2 to 6 MeV/amu.

The target single $K$-vacancy-production cross sections per atom when projectiles are incident with 0, 1, or 2 initial $K$ vacancies may be written in terms of the principal component processes as

$$\begin{aligned}\sigma^0_{SKV}&=\sigma^{i,K\text{-}L}_{SKV},\quad q\le Z_1-3\\ \sigma^1_{SKV}&=\sigma^{i,K\text{-}L}_{SKV}+a\sigma^{K\text{-}K}_{SKV},\quad q=Z_1-1\\ \sigma^2_{SKV}&=\sigma^{i,K\text{-}L}_{SKV}+\sigma^{K\text{-}K}_{SKV},\quad q=Z_1\end{aligned}\tag{1}$$

where $\sigma^{i,K\text{-}L}_{SKV}$ represents the contribution due to direct ionization, excitation, and $K$ electron transfer to the outer shells of the projectile and $\sigma^{K\text{-}K}_{SKV}$ represents the contribution due to target $K$-shell to projectile $K$-shell electron transfer. If we assume that the variation in $\sigma^{i,K\text{-}L}_{SKV}$ with the number of projectile $K$ vacancies is small compared to the enhancement in $\sigma_{SKV}$ for bare and one-electron ions caused by the opening of the target $K$-shell to projectile $K$-shell electron-transfer channel[10] (see Fig. 3), then we may write the transfer cross section $\sigma^{K\text{-}K}_{SKV}$ in terms of the vacancy-production cross sections as

$$\sigma^{K\text{-}K}_{SKV}=\sigma^2_{SKV}-\sigma^0_{SKV}\,.\tag{2}$$

The coefficient $a$ is given by

$$a=\frac{\sigma^1_{SKV}-\sigma^0_{SKV}}{\sigma^2_{SKV}-\sigma^0_{SKV}}\tag{3}$$

and is related to the enhancement in $\sigma_{SKV}$ caused by $K$-to-$K$ electron transfer to a projectile with a single $K$ vacancy. The coefficient $a$ is observed to be $\sim 0.5$ and is approximately independent of projectile velocity over the range relevant to this work. The factor $a$ is useful in estimating cross sections which cannot be measured directly (e.g., $\sigma^2_{SKV}$ at low projectile velocities or $\sigma^0_{SKV}$ at high velocities).

The relative error in experimental values of the $K$-to-$K$ transfer cross section $\sigma^{K\text{-}K}_{SKV}$ is $\sim(25\text{—}35)\%$, primarily due to the fact that Eq. (2) may require measuring a relatively small difference between two large quantities. The absolute error in $\sigma^{K\text{-}K}_{SKV}$ is expected to be $\sim(30\text{—}40)\%$.

The target double $K$-vacancy-production cross sections per atom analogous to Eq. (1) are given by

$$\begin{aligned}\sigma^0_{DKV}&=\sigma^{i,K\text{-}L}_{DKV},\quad q\le Z_1-3\\ \sigma^1_{DKV}&=\sigma^{i,K\text{-}L}_{DKV}+a\sigma^{i,K\text{-}L;K\text{-}K}_{DKV},\quad q=Z_1-1\\ \sigma^2_{DKV}&=\sigma^{i,K\text{-}L}_{DKV}+\sigma^{i,K\text{-}L;K\text{-}K}_{DKV}+\sigma^{2K\text{-}2K}_{DKV},\quad q=Z_1\end{aligned}\tag{4}$$

where $\sigma^{i,K\text{-}L}_{DKV}$ represents the contribution due to all double $K$-vacancy-production processes involving combinations of direct ionization, excitation, and $K$ electron transfer to the outer shells of the projectile, and $\sigma^{i,K\text{-}L;K\text{-}K}_{DKV}$ represents the contribution due to direct ionization, excitation, or $K\rightarrow LMN\ldots$ electron transfer simultaneous with $K$-to-$K$ transfer. Addition of this second term involving single $K$-to-$K$ transfer results in the enhancement of the hypersatellite cross section observed in Fig. 3 for incident one-electron ions. Finally, the cross section $\sigma^{2K\text{-}2K}_{DKV}$ represents the contribution due to double $K$-to-$K$ electron transfer. If we again neglect the variation in $\sigma^{i,K\text{-}L}_{DKV}$ with the number of projectile $K$ vacancies, then $\sigma^{2K\text{-}2K}_{DKV}$ may be expressed in terms of the vacancy-production cross sections as

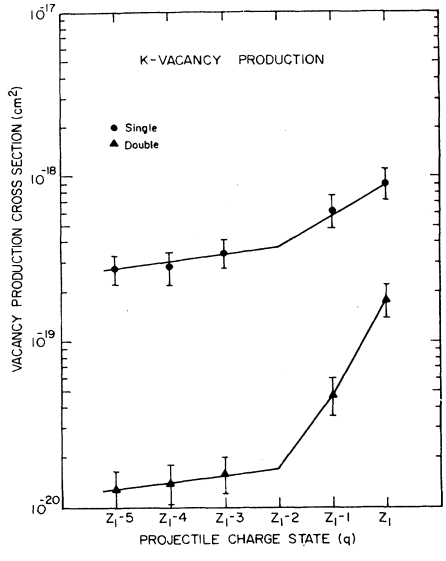


FIG. 3. The charge-state dependences of single $K$-vacancy production $\sigma_{SKV}$ and double $K$-vacancy production $\sigma_{DKV}$ in Ti for 5 MeV/amu $Si^{q+}$ + Ti collisions are presented (reproduced from Ref. 17). The error bars indicate absolute errors in the cross sections. Relative errors are at least a factor of 2 smaller. Cross sections for the two-electron ion beam were not measured due to the metastable $1s\,2s\ ^3S$ component in the beam. The solid lines are eye guides.

$$\sigma_{\mathrm{DKV}}^{2K\text{-}2K}=\sigma_{\mathrm{DKV}}^{2}-\sigma_{\mathrm{DKV}}^{0}-\left[\frac{\sigma_{\mathrm{DKV}}^{1}-\sigma_{\mathrm{DKV}}^{0}}{a}\right]. \quad (5)$$

The relative error in experimental values for $\sigma_{\mathrm{DKV}}^{2K\text{-}2K}$ is $\sim(40\text{—}50)\%$, again due to the fact that Eq. (5) may require measuring relatively small differences between large quantities. The absolute error in $\sigma_{\mathrm{DKV}}^{2K\text{-}2K}$ is expected to be $\sim(45\text{—}55)\%$.

### B. Effective fluorescence yields

The fluorescence yields required to relate x-ray-production cross sections to vacancy-production cross sections are given in general by

$$\omega_K(lm)=\frac{\Gamma_X(lm)}{\Gamma_X(lm)+\Gamma_A(lm)}, \quad (6)$$

where the x-ray and Auger linewidths, $\Gamma_X(lm)$ and $\Gamma_A(lm)$, depend on the electronic configuration of the atom at the instant of decay. In the present work, we assume initial single $K$-vacancy configurations of the form

$$1s^1 2s^2 2p^l 3s^2 3p^m,$$

where, for a given $l$ from 1 to 6, an average value of $m$ has been determined for Ti from the work of Jamison *et al.*[19] The x-ray and Auger linewidths in Eq. (6) represent sums over all allowed x-ray and Auger transitions which lead to filling of the $K$ vacancy. In the absence of a direct calculation, the various linewidths may be estimated using the scaling technique of Larkins.[20] Details of this procedure are discussed elsewhere.[21]

Once the configuration yields $\omega_K(lm)$ have been obtained, the average $K$-shell fluorescence yield $\omega_K$ may be estimated from the intensity distribution of the $K\alpha$ satellite peaks observed in high resolution according to[22]

$$\omega_K=\frac{1}{\sum_{l=1}^{6} I_X^l/\omega_K(lm)}, \quad (7)$$

where $I_X^l$ represents the relative intensity of the satellite peak corresponding to $l$ $L$-shell electrons prior to the decay of the $K$ vacancy. The intensity distribution of the satellite peaks depends upon the degree of multiple $L$-shell vacancy production and therefore on projectile energy. It is not unreasonable to expect that $\omega_K$ should reflect this energy dependence. Figure 4 shows the energy dependence of $\omega_K$ calculated from Eq. (7) using relative satellite intensities of Sc (Ref. 23) (open points) and Ti (Refs. 19, 24, and 25) (closed points) and $\omega_K(lm)$ values detailed in Ref. 21. For light ions, where there is little multiple $L$-shell vacancy production, the energy dependence is flat. However, for heavy ions there is a peak in $\omega_K$ near matched velocity for the Ti $L$ shell ($\sim$1 MeV/amu), the point at which $L$-shell vacancy production is maximized. The dashed line in Fig. 4 represents an average value of $\omega_K$ for incident heavy ions and will be the value used in this work.

In order to determine $K$-to-$K$ electron-transfer cross sections via Eqs. (2) and (5), it is necessary to know the dependence of the target fluorescence yield on the charge state of the incident projectile. This was investigated in the work of Tawara *et al.*[26] in which the average fluorescence yield of Si bombarded by F ions was studied as a function of both the charge states of the projectile and the physical state of the target. The average fluorescence yield for $SiH_4$ gas targets was observed to increase with the projectile charge state, reflecting the fact that outer-shell vacancies formed in a gaseous target are not filled from the local environment prior to decay of the $K$ vacancy. The relatively higher electron density within a solid target allows outer-shell vacancies to be filled prior to inner-shell decay, and no dependence of $\omega_K$ on the projectile charge state is observed.

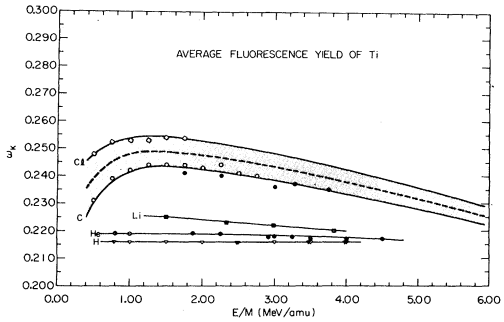


FIG. 4. Average Ti fluorescence yields calculated from Eq. (7) using relative $K\alpha$ satellite intensities of Sc (Ref. 23) (open points) and Ti (Refs. 19, 24, and 25) (closed points) and $\omega_K(lm)$ values detailed in Ref. 21. The shaded region contains additional data (not explicitly shown) for N, O, and F up to $\sim$3 MeV/amu. Above 3 MeV/amu, the curve is a smooth extrapolation back down to $\omega_K$ for $H^+$.

Earlier, the assumption was made that the hypersatellite fluorescence yield was equal to the average $K$-shell fluorescence yield $\omega_K$. Recent calculations by Tunnell and Bhalla[27] for multiply ionized systems in the range $7\leq Z\leq 14$ indicate that when the $L$ shell is more than half full ($l\geq 4$) the ratios of the hypersatellite fluorescence yield to the satellite fluorescence yield for a given initial configuration are relatively constant to within 5% of 0.905 and show no significant dependence on atomic number. For higher multiple ionization states ($l\leq 3$) the ratios become consistently smaller ($\lesssim$0.750) with slight increases noted for increasing atomic number. However, this deviation does not significantly affect our original assumption since these latter configurations are only weakly populated in the range of heavy-ion—atom collisions considered here.[23] It should also be noted that there exist no direct experimental values for hypersatellite fluorescence yields in heavy ions. More work is needed here.

A reasonable estimate for the error in $\omega_K$ is $\sim(10\text{—}15)\%$ given absolute errors in the relative satellite intensities of $\sim(5\text{—}10)\%$ and errors in the $\omega_K(lm)$ of $\sim 10\%$. The error introduced by equating the hypersatellite fluorescence yield to the average $K$-shell fluorescence yield is difficult to estimate but may be $\sim(20\text{—}25)\%$.

## IV. THEORETICAL MODELS

One of the most extensively studied mechanisms for producing inner-shell vacancies in ion-atom collisions is direct Coulomb ionization. The simplest theoretical model for ionization is the plane-wave Born approximation (PWBA).[3] In the PWBA, the initial and final states

of the projectile are assumed to be plane waves with momentum vectors $\vec{K}_i$ and $\vec{K}_f$ which differ by an amount equal to the momentum transferred to a target electron. The initial- and final-state wave functions of the active electron are typically represented by discrete and continuum screened hydrogenic wave functions, respectively. The use of more complex multielectron wave functions to describe the target electronic configuration is avoided by adopting the independent-electron approximation. In the independent-electron approximation, all of the electrons, except the one undergoing a transition, are assumed to be passive spectators in the collision. Their function is to screen the Coulomb interaction between the active electron and the target and projectile nuclei. In the PWBA, the Coulomb interaction between the projectile and the active electron is assumed to be weak enough to allow the use of a first-order perturbation approximation. The PWBA predicts a $Z_1^2$ scaling of the ionization cross section at a fixed projectile velocity.

In their standard form, PWBA calculations for $K$-shell ionization are equivalent to using a straight-line projectile trajectory in the semiclassical approximation and rely on the assumption that the projectile-electron interaction time is short compared with the electron response time. Depending upon the scaled velocity of the projectile, these conditions may not be realized in a particular collision system. In the low-velocity regime ($v_1 \ll v_{2K}$), where ionization is expected to occur primarily on deep penetration by the projectile to internuclear distances much less than the target $K$-shell radius,[2] PWBA cross sections overestimate experimental values by as much as two orders of magnitude. To account for this discrepancy, Basbas *et al.*[6] have utilized a perturbed stationary-state approach to incorporate the effects of Coulomb deflection ($C$) and increased target $K$-shell binding energy ($B$) into the PWBA. These effects give rise to subtractive corrections proportional to $Z_1^3$ which decrease the cross sections and bring about improved agreement between experimental data and theory for ionization by $H^+$ ions at low projectile velocities. However, these calculations underestimate cross sections for ionization by heavier ions. In the intermediate velocity regime ($v_1 \sim v_{2K}$), where the dominant contribution to ionization is made by projectiles penetrating to internuclear distances on the order of the target $K$-shell radius,[2] polarization effects may become important. In recent work, Basbas *et al.*[7] have extended their previous calculations to include the effects of target $K$-shell polarization ($P$) by the projectile. Polarization results in a distortion of the electron orbit which decreases the effective target $K$-shell binding energy by increasing the average $K$-shell radius. This is manifested in the calculated cross sections as an additive $Z_1^3$ effect which extends agreement with experiment up through collision partners with $Z_1/Z_2 \lesssim 0.3$ and $v_1/v_{2K} \lesssim 2$.[7] In addition, these calculations introduce a radial cutoff parameter into the computation of the binding energy correction and the polarization correction. In the high-velocity regime ($v_1 \gg v_{2K}$), the $C$, $B$, and $P$ corrections to the PWBA subside and the cross sections become asymptotically proportional to $Z_1^2$.

Inner-shell vacancies may also be produced by the transfer of electrons from initial bound states of the target to final bound or continuum states of the projectile. Traditional formulations used to describe the transfer process in the high-velocity regime have been based on first-order perturbation theory. However, for near-symmetric collisions ($Z_1 \sim Z_2$) in the low- to intermediate-velocity regime ($v_1 \lesssim v_{2i}$), the transfer probability is not small and the perturbation approach is no longer valid. In this region, where electron transfer is dominated by contributions from impact parameters comparable to or greater than the average orbital radius of the electron in its initial state, Lin *et al.*[8] have shown that a nonperturbative two-center atomic-expansion model provides a convenient basis for describing the transfer process. For the case of $K$-shell—to—$K$-shell transfer in an independent electron approximation, the time evolution of the two-electron wave function can be expanded in terms of three *atomic* eigenstates: (1) the initial two-electron state centered about the target, (2) the final two-electron transfer state centered about the projectile, and (3) an intermediate state in which only one electron has been transferred. This close-coupling expansion results in a set of time-dependent coupled equations which can be solved to obtain single and double $K$-shell—to—$K$-shell electron-transfer probabilities. If the intermediate state is properly symmetrized with respect to the interchange of the two electrons, it can be demonstrated that both of these transfer probabilities follow binomial distributions, i.e., that the single electron-transfer probability at each impact parameter is given by $P_1 = 2(1-P)P$ and the double electron-transfer probability is given by $P_2 = P^2$ where $P$ is the electron transfer probability calculated in the *one-electron* two-center, two-state atomic-expansion (TSAE) model[8] (see the Appendix for details). Thus the TSAE calculation allows one to obtain single as well as double $K$-shell—to—$K$-shell electron-transfer cross sections so long as electron-electron correlation effects are neglected.

For asymmetric collisions in which the projectile nuclear charge $Z_1$ is much smaller than the target charge $Z_2$, the electron-transfer probability is small. In this case, Reading, Ford, and Becker[9] have shown that the time-dependent wave function for the active electron can be well represented by a one-center, multistate expansion about the target plus an appropriate projectile-centered final state. This type of expansion allows one to derive transition amplitudes to bound and continuum states of the target along with small-amplitude electron transfer to the projectile.

While there are other approaches to the calculation of electron transfer (e.g., Lapicki and McDaniel[28]), in this work we restrict the comparison of theory and experiment to *ab initio* calculations.

## V. DISCUSSION

### A. Single K-vacancy production

The projectile energy and $Z_1$ dependences of single $K$-vacancy production are shown in Figs. 5 and 6, respectively, for representative cases. Owing to space limitations, a complete tabulation of our experimental data (approximately 750 cross sections) is provided elsewhere.[29] Experimental points are derived from primary satellite x-ray-production cross sections for projectiles incident with zero (●) and two (▲) initial $K$-shell vacancies. The range of measured cross sections shown in Fig. 6 has been extended

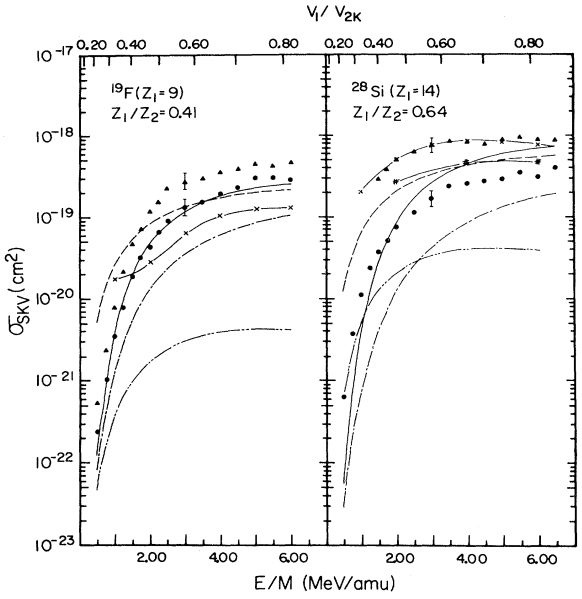


FIG. 5. Representative energy dependences of single $K$-vacancy production for bare and multielectron projectiles. The measured cross sections are $\sigma^0_{SKV}$ (●) and $\sigma^2_{SKV}$ (▲). Representative error bars are shown. The calculated cross sections represent PWBA (— — —), PWBA (*CB*) (—·—·—·), PWBA (*CBP*) (——), Reading *et al.* (Ref. 9) (—#—#—), TSAE $K\rightarrow K$ transfer (—×—×—), and scaled OBK $K\rightarrow LMN\ldots$ transfer (—··—··—··).

down to $Z_1/Z_2\sim 0.05$ ($Z_1=1$) by including data for H ions from Khan *et al.*,[11] He from McDaniel *et al.*[12] and Soares *et al.*[13], Li from McDaniel *et al.*,[14] and B from Monigold *et al.*[15] Where necessary, data points have either been interpolated from the literature or estimated from the present work using Eq. (3). The theoretical curves represent PWBA (— — —), PWBA(*CB*) (—·—·—·), and PWBA(*CBP*) (——) cross sections for direct ionization calculated from the program XCODE.[30] The one-center, multistate calculation of Reading *et al.*[9] (—#—#—) is included for the case of Si + Ti. Also shown are scaled OBK cross sections[4] (—··—··—··—) for electron transfer from the target $K$ shell to outer shells of the projectile and TSAE calculations[8] (—×—×—) for single $K$-to-$K$ electron transfer. The OBK calculations have been scaled by a factor of $\frac{1}{30}$ to facilitate comparison with measured cross sections.

Compared with the present work, PWBA(*CBP*) calculations appear to adequately predict the observed energy and $Z_1$ dependences of single $K$-vacancy production by multielectron ions ($\sigma^0_{SKV}$; $q\leq Z_1-3$) up through collision systems with $Z_1/Z_2\sim 0.40$ ($Z_1=9$). Beyond this, PWBA(*CBP*) calculations tend increasingly to underestimate measured cross sections at low scaled velocities ($v_1/v_{2K}\lesssim 0.50$) and overestimate for higher velocities. The systematic nature of the deviation at low velocities is easily seen in Fig. 6. In contrast with uncorrected PWBA calculations, which increase monotonically as $Z_1^2$ for all projectile velocities, PWBA(*CB*) and PWBA(*CBP*) calculations exhibit a turnover in their $Z_1$ dependence at low

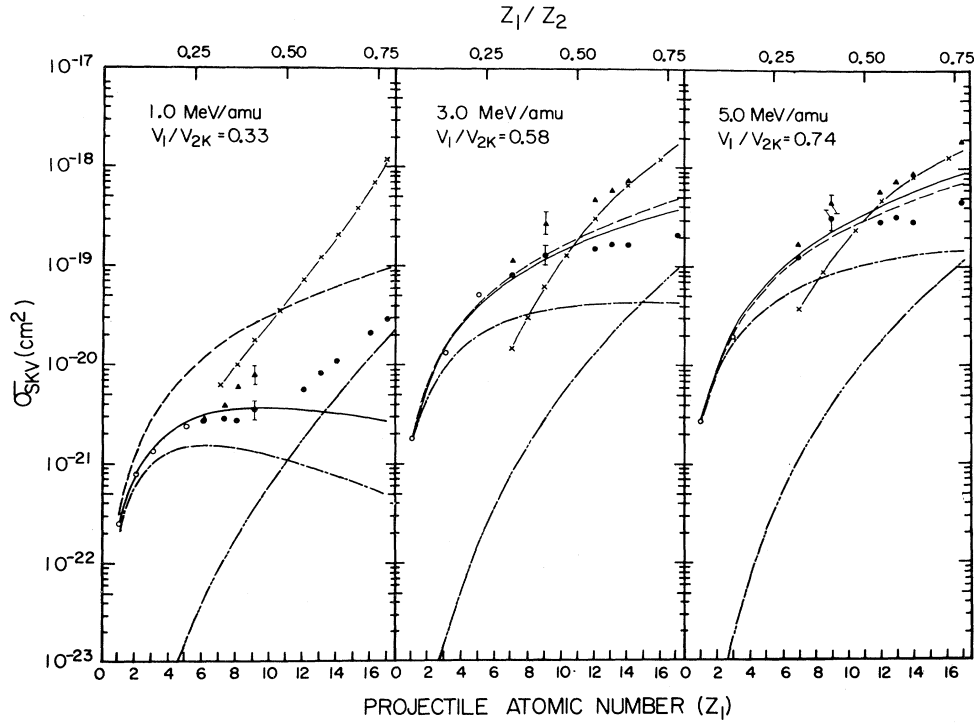


FIG. 6. Representative $Z_1$ dependences of single $K$-vacancy production for bare and multielectron projectiles. The measured cross sections are $\sigma^0_{SKV}$ (●) and $\sigma^2_{SKV}$ (▲). Values from the literature (○) include H from Khan *et al.* (Ref. 11), He from McDaniel *et al.* (Ref. 12) and Soares *et al.* (Ref. 13), Li from McDaniel *et al.* (Ref. 14), and B from Monigold *et al.* (Ref. 15). Representative error bars are shown. The calculated cross sections represent PWBA (— — —), PWBA(*CB*) (—·—·—·), PWBA(*CBP*) (——), TSAE $K\rightarrow K$ transfer (—×—×—), and scaled OBK $K\rightarrow LMN\ldots$ transfer (—··—··—··).

scaled velocities reflecting the dominance of subtractive $Z_1^3$ effects associated primarily with binding energy corrections. The upturn in the $Z_1$ dependence of the experimental cross section at low velocities for $Z_1/Z_2 \gtrsim 0.40$ is attributed to the onset of $K \rightarrow LMN \ldots$ electron transfer. For $v_1/v_{2K} \lesssim 0.50$ and $Z_1/Z_2 \gtrsim 0.40$, the qualitative trends in the observed $Z_1$ dependence can be reproduced by combining scaled OBK electron-transfer calculations with PWBA(*CBP*) calculations for direct ionization. However, at higher velocities, where single $K$-vacancy production by multielectron ions is dominated by direct ionization in all but near-symmetric collision systems ($Z_1 \sim Z_2$), PWBA(*CBP*) calculations continue to overestimate measured cross sections by up to a factor of 2, and the observed $Z_1$ dependence cannot be reproduced. The multistate calculation of Reading *et al.*[9] was performed for incident ions with a filled $K$ shell and already includes a contribution due to $K \rightarrow LMN \ldots$ electron transfer. It predicts a flatter energy dependence than observed and overestimates experimental cross sections by factors of 2–3 for the case of Si + Ti. PWBA(*CB*) calculations tend to underestimate measured $\sigma^0_{SKV}$ cross sections for the collision systems considered in this work.

Single $K$-vacancy production by bare ions ($\sigma^2_{SKV}$) shows a marked enhancement over that observed for multielectron ions ($\sigma^0_{SKV}$). The two cross sections show a similar energy dependence but the data for bare ions have a steeper $Z_1$ dependence. The difference between the two cross sections is attributed to the addition of the $K$-to-$K$ electron transfer channel. For $v_1/v_{2K} \gtrsim 0.40$ and $Z_1/Z_2 \gtrsim 0.50$, the region in which TSAE calculations are expected to be valid, the qualitative trends in the energy and $Z_1$ dependences of measured $\sigma^2_{SKV}$ cross sections can be reproduced by combining the contributions from direct ionization and electron transfer to all shells of the projectile. Although the effects are most pronounced in near-symmetric collision systems, $K$-to-$K$ electron transfer appears to make a significant contribution to single $K$-vacancy production by bare ions in collision systems as low as

$$Z_1/Z_2 \sim 0.25 \ (Z_1 = 6) \ .$$

The systematics of $K$-to-$K$ electron transfer are shown in Figs. 7 and 8 for representative cases. Experimental points are derived from primary satellite x-ray-production cross sections according to Eq. (2). The theoretical curves represent the TSAE calculations of Lin *et al.*[8] (—×—×—), and unscaled OBK (Ref. 4) (— — —) calculations for $K$-to-$K$ electron transfer. The one-center, multistate calculation of Reading *et al.*[9] (—#—#—) is included for the case of Si + Ti.

The energy dependence of the measured $K$-to-$K$ electron-transfer cross sections shows a steep rise with increasing velocity at low scaled velocities but tends to flatten into a broad plateau for $v_1/v_{2K} \gtrsim 0.50$. The plateau extends to increasingly lower velocities as more nearly symmetric collision systems are approached. For $v_1/v_{2K} \gtrsim 0.40$ and $Z_1/Z_2 \gtrsim 0.50$, TSAE calculations are in reasonable agreement with both the observed energy dependence and general magnitude of the measured cross sections. For more asymmetric systems, TSAE calculations tend to underestimate experimental cross sections at

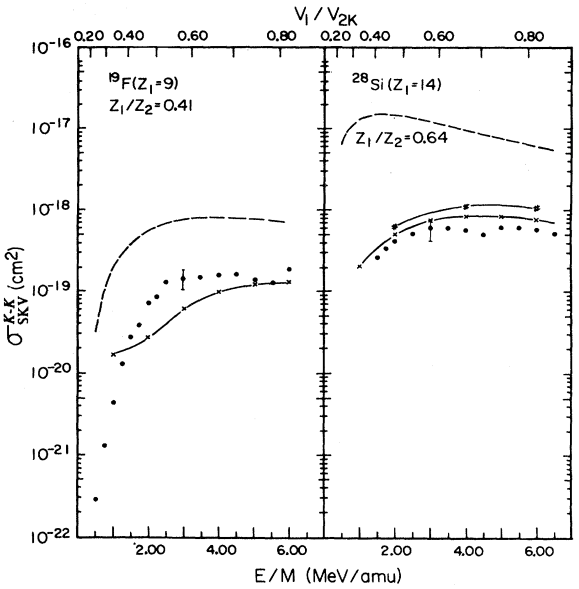


FIG. 7. Representative energy dependences of single $K$-to-$K$ electron transfer. The measured cross sections are $\sigma^{K\text{-}K}_{SKV}$ (●). Representative error bars are shown. The calculated cross sections represent TSAE (—×—×—), Reading *et al.* (Ref. 9) (—#—#—), and unscaled OBK (— — —).

all but the lowest velocities where the upturn in the calculation is an artifact of the breakdown of the approximation. The $Z_1$ dependence of the measured cross sections rises rapidly for low scaled velocities but tapers off some-

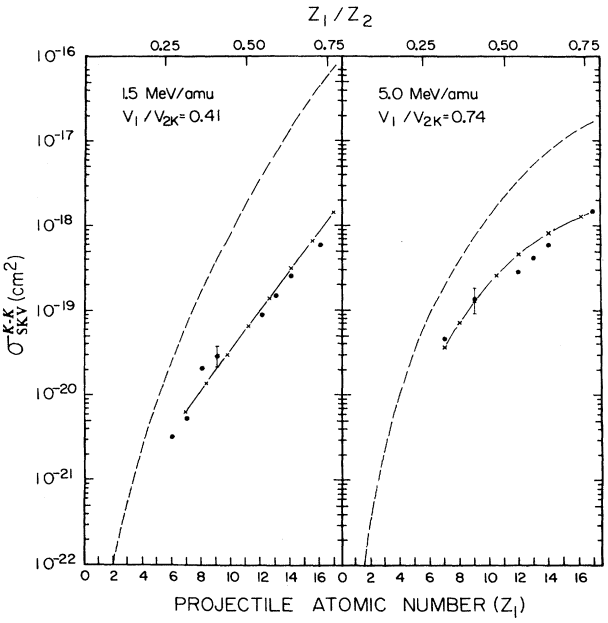


FIG. 8. Representative $Z_1$ dependence of single $K$-to-$K$ electron transfer. The measured cross sections are $\sigma^{K\text{-}K}_{SKV}$ (●). Representative error bars are shown. The calculated cross sections represent TSAE (—×—×—), and unscaled OBK (— — —).

what at higher velocities. Again, TSAE calculations show reasonable agreement with the observed $Z_1$ dependence and general magnitude of the experimental data for $v_1/v_{2K} \gtrsim 0.40$ and $Z_1/Z_2 \gtrsim 0.50$. The calculations of Reading *et al.*,[9] shown only for the case of Si + Ti, overestimate experimental cross sections by $\sim 50\%$ but show reasonable agreement with the observed energy dependence.

Depending on the collision system, $K$-to-$K$ electron transfer may be comparable in magnitude to the sum of the other $K$-shell-vacancy-production mechanisms. $K$-to-$K$ transfer cross sections tend to rise more rapidly with $Z_1$ than $\sigma^0_{SKV}$ cross sections (cf. Figs. 6 and 8) and are observed to exceed $\sigma^0_{SKV}$ for $Z_1/Z_2 \gtrsim 0.40$. Measured $K$-to-$K$ electron-transfer cross sections for incident bare ions, $\sigma^{K\text{-}K}_{SKV}$, exceed $\sigma^0_{SKV}$ by factors of 5—10 for some near-symmetric collision systems at low scaled velocities.

### B. Double $K$-vacancy production

The projectile energy and $Z_1$ dependences of double $K$-vacancy production are shown in Fig. 9 for a representative case. Experimental points are derived from $K\alpha$ hypersatellite x-ray-production cross sections for projectiles incident with zero (●) and two (▲) initial $K$-shell vacancies. The one-center, multistate calculation of Reading *et al.*[9] (—#—#—) is shown for the case of Si + Ti.

Experimental double $K$-vacancy-production cross sections fall one to two orders of magnitude below those observed for single $K$-vacancy production, although the two processes show generally similar systematics. Measured $\sigma^0_{DKV}$ and $\sigma^2_{DKV}$ cross sections tend to increase more rapidly with $Z_1$ than do the corresponding cross sections for single $K$-vacancy production. For the case of $\sigma^0_{DKV}$, this can be attributed to the addition of processes involving not only double $K \rightarrow LMN\ldots$ electron transfer, but also direct ionization simultaneous with single $K \rightarrow LMN\ldots$ transfer. The steeper $Z_1$ dependence of $\sigma^2_{DKV}$ can be associated with two additional processes: (1) direct ionization or $K \rightarrow LMN\ldots$ electron transfer, simultaneous with single $K$-to-$K$ transfer, and (2) double $K$-to-$K$ electron transfer, which increases even more rapidly with $Z_1$ than does single $K$-to-$K$ transfer.[16,17] The observed energy dependence for $\sigma^0_{DKV}$ and $\sigma^2_{DKV}$ is also somewhat steeper than for single $K$-vacancy production. The calculations of Reading *et al.*,[9] which include contributions from all two-electron processes leading to double $K$-vacancy production, overestimate measured $\sigma^2_{DKV}$ cross sections by $\sim 50\%$ for the case of Si + Ti but show reasonable agreement with the observed energy dependence.

The systematics of double $K$-to-$K$ electron transfer are shown in Fig. 10 for a representative case. Experimental points are derived from hypersatellite x-ray-production cross sections according to Eq. (5). The theoretical curves represent the TSAE calculations of Lin *et al.*[8] (—×—×—) and the one-center, multistate calculation of Reading *et al.*[9] (—#—#—).

Experimental cross sections for double $K$-to-$K$ electron transfer again fall one to two orders of magnitude below those observed for single $K$-to-$K$ transfer. Measured $\sigma^{2K\text{-}2K}_{DKV}$ cross sections are observed to rise more rapidly with $Z_1$ than corresponding $\sigma^{K\text{-}K}_{SKV}$ cross sections. The broad plateau observed in the energy dependence of the single $K$-to-$K$ transfer cross section is not seen for double $K$-to-$K$ transfer. For $v_1/v_{2K} \gtrsim 0.40$ and $Z_1/Z_2 \gtrsim 0.50$,

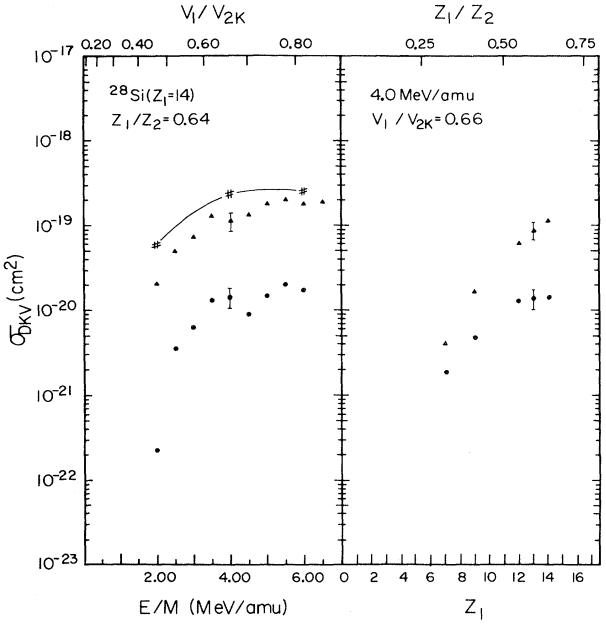


FIG. 9. Representative energy and $Z_1$ dependence of double $K$-vacancy production for bare and multielectron projectiles. The measured cross sections are $\sigma^0_{DKV}$ (●) and $\sigma^2_{DKV}$ (▲). Representative error bars are shown. The calculated cross sections represent Reading *et al.* (Ref. 9) (—#—#—).

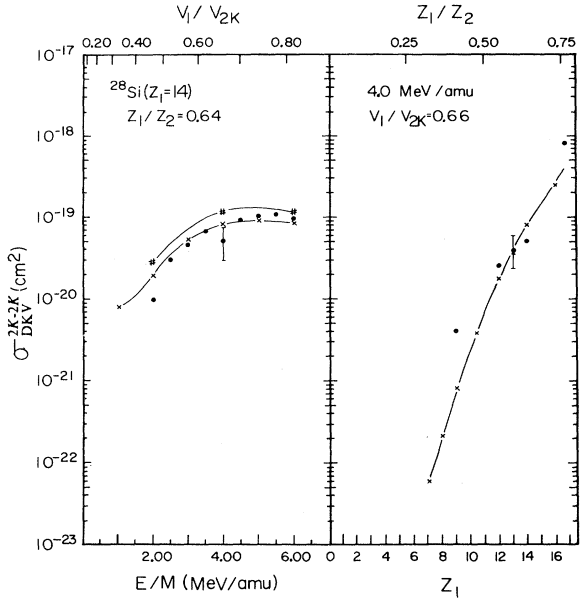


FIG. 10. Representative energy and $Z_1$ dependence of double $K$-to-$K$ electron transfer. The measured cross sections are $\sigma^{2K\text{-}2K}_{DKV}$ (●). Representative error bars are shown. The calculated cross sections represent TSAE (—×—×—) and Reading *et al.* (Ref. 9) (—#—#—).

TSAE calculations are in reasonable agreement with the observed energy and $Z_1$ dependences and the general magnitude of the experimental data. The results of the multistate calculations of Reading *et al.*[9] are also in reasonable agreement with experimental data for the case of Si + Ti.

Double $K$-to-$K$ transfer cross sections are observed to exceed $\sigma^0_{DKV}$ for $Z_1/Z_2 \gtrsim 0.50$. Measured double $K$-to-$K$ electron transfer cross sections for bare incident ions, $\sigma^{2K\text{-}2K}_{DKV}$, exceed $\sigma^0_{DKV}$ by up to a factor of $\sim 100$ for some near-symmetric collision systems at low scaled velocities.

## VI. SUMMARY

The present work provides a broad range of self-consistent data for direct Coulomb ionization and $K$-shell—to—K-shell electron transfer in the low- to intermediate-velocity regime. Apart from the Auger data of Woods *et al.*[31] for N, O, and F incident on Ne, the measurements presented here represent the only available heavy-ion data for double $K$-to-$K$ transfer.

Direct ionization was found to play a dominant role in target $K$-shell-vacancy production by multielectron projectiles ($q \leq Z_1 - 3$) in systems with $Z_1/Z_2 \lesssim 0.40$ and $v_1/v_{2K} \lesssim 0.50$. As $Z_1/Z_2$ increases towards unity (symmetric systems), $K \rightarrow LMN\ldots$ electron transfer is found to play an increasingly important role in $K$-vacancy production. As $v_1/v_{2K}$ increases towards unity (matched velocity), direct ionization appears to dominate in all but near-symmetric systems ($Z_1/Z_2 \gtrsim 0.75$). For the case of bare incident ions ($q = Z_1$), $K$-to-$K$ electron transfer was found to make a significant contribution to target $K$-vacancy production in systems as low as $Z_1/Z_2 \sim 0.25$. It was noted that the rates of both single and double $K$-to-$K$ electron transfer may increase to a level one to two orders of magnitude larger than the respective sums of the other $K$-shell-vacancy-production mechanisms for some near-symmetric collision systems ($Z_1/Z_2 \gtrsim 0.75$) at low to intermediate scaled velocities ($v_1/v_{2K} \lesssim 0.50$).

The agreement between theory and experiment for three of the principal models for inner-shell vacancy production is summarized in Figs. 11—13. The figures depict the ratio of the experimental cross section to the calculated cross section for the cases of direct ionization compared to the PWBA(*CBP*), single $K$-to-$K$ electron transfer compared to the TSAE, and double $K$-to-$K$ electron transfer compared to the TSAE. Figure 11 shows that PWBA(*CBP*) calculations give reasonable agreement with experiment in asymmetric collision systems ($Z_1/Z_1 \lesssim 0.40$). For more symmetric systems, PWBA(*CBP*) calculations underestimate measured cross sections at low scaled velocities ($v_1/v_{2K} \lesssim 0.50$) and overestimate the cross sections for higher velocities. The deviation at the lower velocities is associated with the onset of $K \rightarrow LMN\ldots$ electron transfer. Figure 12 shows that TSAE calculations give reasonable agreement with experiment in collision systems with $Z_1/Z_2 \gtrsim 0.50$ and $v_1/v_{2K} \gtrsim 0.40$. For more asymmetric systems, TSAE calculations tend to underestimate measured $K$-to-$K$ electron-transfer cross sections at all but the lowest velocities where the downturn in the ratio reflects the onset of molecular effects not described by a two-state atomic-expansion model. Molecular effects and their influence on the validity of the TSAE approximation have been investigated recently in a modified multistate

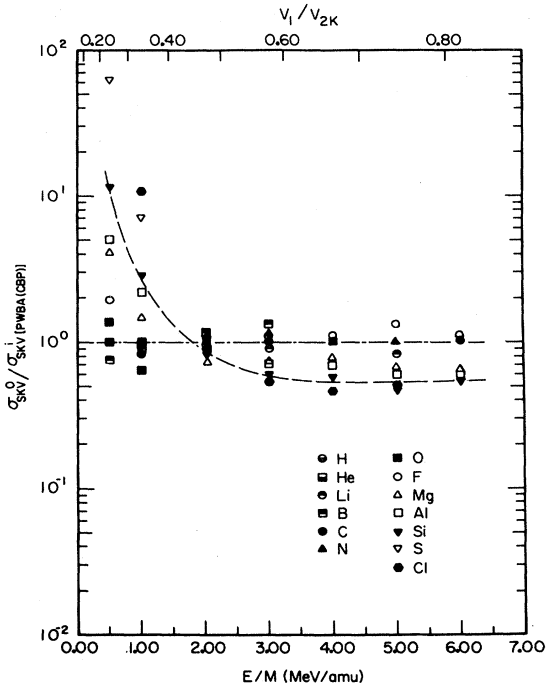


FIG. 11. Ratio of $\sigma^0_{SKV}/\sigma^i_{SKV}$ [PWBA(*CBP*)] showing typical asymmetric (—·—·—·) and near-symmetric (— — —) behavior. Values from the literature include H from Khan *et al.* (Ref. 11), He from McDaniel *et al.* (Ref. 12), and Soares *et al.* (Ref. 13), Li from McDaniel *et al.* (Ref. 14), and B from Monigold *et al.* (Ref. 15).

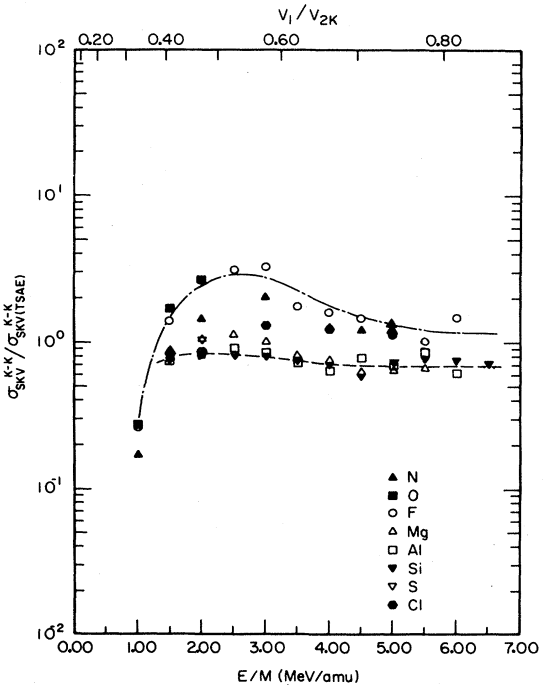


FIG. 12. Ratio of $\sigma^{K\text{-}K}_{SKV}/\sigma^{K\text{-}K}_{SKV\,(TSAE)}$ showing typical asymmetric (—·—·—·) and near-symmetric (— — —) behavior.

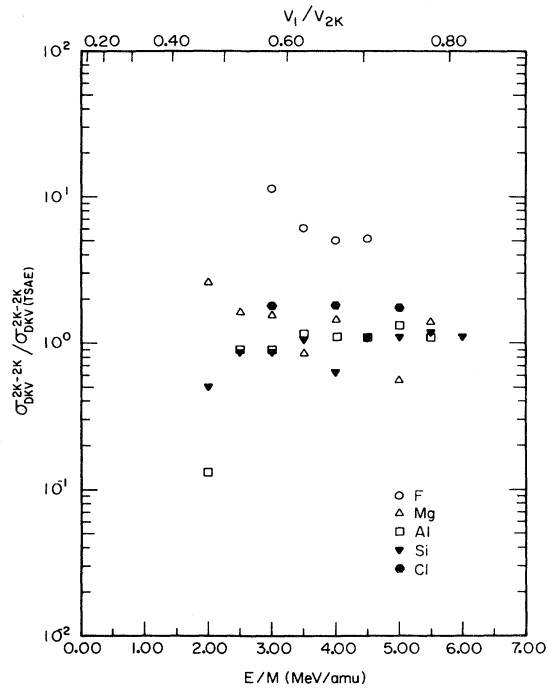


FIG. 13. Ratio of $\sigma^{2K\text{-}2K}_{DKV}/\sigma^{2K\text{-}2K}_{DKV(TSAE)}$.

atomic-expansion model by Fritsch and Lin[32] for true one-electron ion-atom collision systems. Figure 13 shows that TSAE calculations give reasonable agreement with experimental double $K$-to-$K$ electron-transfer cross sections in collision systems with $Z_1/Z_2 \gtrsim 0.50$ and $v_1/v_{2K} \gtrsim 0.40$. For more asymmetric systems, substantial deviations from theory arise.

The present work has suggested a need for further investigation in two areas. (1) Although the present work covers a broad range of scaled collision velocities, recent advances in accelerator technology make it possible to extend the range of the present work to both higher and lower collision velocities. Extending the range to lower velocities would make it possible to study the transition between "atomic" and "molecular" descriptions of inner-shell vacancy production. Extending the range to higher velocities would access the region of matched collision velocity for the target $K$ shell ($v_1 \sim v_{2K}$) where many of the vacancy production mechanisms are expected to be maximized. (2) The double $K$-vacancy-production cross sections presented in this work are sensitive to the value of the hypersatellite fluorescence yield—a quantity which has yet to be experimentally measured. This points to a need for experiments in which both the x-ray and Auger hypersatellites are investigated for a given system.

## ACKNOWLEDGMENTS

The authors would like to express their appreciation to J. F. Reading and A. L. Ford for providing some of the calculations presented in this work prior to publication. This work was supported by the Division of Chemical Sciences, U. S. Department of Energy.

## APPENDIX: DERIVATION OF THE BINOMIAL DISTRIBUTIONS OF SINGLE AND DOUBLE ELECTRON-TRANSFER PROBABILITIES IN A COUPLED ATOMIC-STATE EXPANSION

Consider a model system which consists of two independent, indistinguishable electrons in the field of both the target nucleus and a bare projectile. The model Hamiltonian for the system is assumed to be of the form

$$H_{el} = -\tfrac{1}{2}\nabla_1^2 - \tfrac{1}{2}\nabla_2^2 + V_T(r_{1T}) + V_T(r_{2T}) + V_P(r_{1P}) + V_P(r_{2P}) , \tag{A1}$$

where the index $i=1,2$ refers to the electrons, $r_{iA}$ is the separation between electron $i$ and nucleus $A$, and $V_T$ ($V_P$) is the effective potential due to the target (projectile). The electron-electron Coulomb repulsion is assumed to provide some screening which is included in the model potential $V_T$ ($V_P$). Since the model Hamiltonian is separable with respect to the two electrons,

$$H_{el} = h_{el}(1) + h_{el}(2) , \tag{A2}$$

an eigenstate of the two-electron Hamiltonian is the product of eigenstates of the one-electron Hamiltonian,

$$h_{el} = -\tfrac{1}{2}\nabla^2 + V_T(r_T) + V_P(r_P) . \tag{A3}$$

In considering the electron-transfer process for the model system, the initial state of the two electrons (bound to the target nucleus) may be described in terms of the product wave function $\phi_i(\vec{r}_{1T})\phi_i(\vec{r}_{2T})$ where $\phi_i(\vec{r}_T)$ satisfies

$$[-\tfrac{1}{2}\nabla^2 + V_T(r_T) - \epsilon_i]\phi_i(\vec{r}_T) = 0 . \tag{A4}$$

For the case of double electron transfer, the final state of the system is $\phi_f(\vec{r}_{1P})\phi_f(\vec{r}_{2P})$ where $\phi_f(\vec{r}_P)$ satisfies

$$[-\tfrac{1}{2}\nabla^2 + V_P(r_P) - \epsilon_f]\phi_f(\vec{r}_P) = 0 . \tag{A5}$$

In these expressions, $\epsilon_i$ ($\epsilon_f$) is the eigenenergy of the electron in its initial (final) state. For single transfer, the symmetrized product wave function is

$$\phi_i(\vec{r}_{1T})\phi_f(\vec{r}_{2P}) + \phi_f(\vec{r}_{1P})\phi_i(\vec{r}_{2T}) .$$

Since the target and projectile centers are moving with velocities $-\vec{v}/2$ and $\vec{v}/2$, respectively, with respect to the midpoint of the internuclear axis, which was taken to be the origin of the coordinate system, the time-dependent wave function for the two electrons may be expanded in a truncated basis as

$$\Psi(\vec{r}_1,\vec{r}_2,t)=A(t)\phi_i(\vec{r}_{1T})\phi_i(\vec{r}_{2T})\exp[-i(\tfrac{1}{2}\vec{v}\cdot\vec{r}_1+\tfrac{1}{2}\vec{v}\cdot\vec{r}_2+\tfrac{1}{4}v^2t+2\epsilon_i t)]$$
$$+B(t)(\phi_f(\vec{r}_{1P})\phi_i(\vec{r}_{2T})\exp\{-i[-\tfrac{1}{2}\vec{v}\cdot\vec{r}_1+\tfrac{1}{2}\vec{v}\cdot\vec{r}_2+\tfrac{1}{4}v^2t+(\epsilon_i+\epsilon_f)t]\}$$
$$+\phi_i(\vec{r}_{1T})\phi_f(\vec{r}_{2P})\exp\{-i[\tfrac{1}{2}\vec{v}\cdot\vec{r}_1-\tfrac{1}{2}\vec{v}\cdot\vec{r}_2+\tfrac{1}{4}v^2t+(\epsilon_i+\epsilon_f)t]\})$$
$$+C(t)\phi_f(\vec{r}_{1P})\phi_f(\vec{r}_{2P})\exp[-i(-\tfrac{1}{2}\vec{v}\cdot\vec{r}_1-\tfrac{1}{2}\vec{v}\cdot\vec{r}_2+\tfrac{1}{4}v^2t+2\epsilon_f t)]\ . \tag{A6}$$

It is straightforward to see that the time evolution of the two-electron wave function (A6) is the product of the time-dependent wave functions of the two independent electrons. To see this, recall that the time evolution of each electron is governed by

$$\left[h_{\rm el}-i\frac{\partial}{\partial t}\right]\Phi(\vec{r},t)=0\ , \tag{A7}$$

where

$$\Phi(\vec{r}_1,t)=a(t)\phi_i(\vec{r}_{1T})\exp[-i(\tfrac{1}{2}\vec{v}\cdot\vec{r}_1+\tfrac{1}{8}v^2t+\epsilon_i t)]$$
$$+b(t)\phi_f(\vec{r}_{1P})\exp[-i(-\tfrac{1}{2}\vec{v}\cdot\vec{r}_1+\tfrac{1}{8}v^2t+\epsilon_f t)]\ , \tag{A8}$$

and similarly for $\Phi(\vec{r}_2,t)$. The two-electron wave function may then be written as

$$\Psi(\vec{r}_1,\vec{r}_2,t)=\Phi(\vec{r}_1,t)\Phi(\vec{r}_2,t)$$

with the following definitions:

$$A(t)=a^2(t)\ ,$$
$$B(t)=a(t)b(t)\ , \tag{A9}$$
$$C(t)=b^2(t)\ ,$$

where $a(t)$ and $b(t)$ are obtained by solving the one-electron Schrödinger equation (A7) in the two-center, two-state atomic-expansion (TSAE) model.[8] From (A6) and (A9), the single-transfer probability is found to be

$$P_1=2\,|B(+\infty)|^2$$
$$=2\,|a(+\infty)|^2\,|b(+\infty)|^2$$
$$=2(1-P)P \tag{A10}$$

while the double-transfer probability is

$$P_2=|C(+\infty)|^2=P^2\ , \tag{A11}$$

where we have defined $P=|b(+\infty)|^2$.

This conclusion appears to be obvious, but the derivation illustrates the assumptions used in the model. This derivation differs from the earlier work of Lin *et al.*[8] by requiring that the wave function (A6) be properly symmetrized with respect to interchange of the two electrons.

*Present address: Physics Division, Oak Ridge National Laboratory, Oak Ridge, Tennessee 37830.

[1]J. D. Garcia, E. Gerjuoy, and J. E. Welker, Phys. Rev. 165, 66 (1968).

[2]J. Bang and J. M. Hansteen, K. Dan. Vidensk. Selsk. Mat.—Fys. Medd. 31, No. 13 (1959).

[3]E. Merzbacher and H. W. Lewis, *Handbuch der Physik,* edited by S. Flügge (Springer, Berlin, Göttingen, Heidelberg, 1958), Vol. 34, pp. 166—192.

[4]V. S. Nikolaev, Zh. Eksp. Teor. Fiz. 51, 1263 (1966) [Sov. Phys.—JETP 24, 847 (1967)].

[5]J. D. Garcia, R. J. Fortner, and T. M. Kavanagh, Rev. Mod. Phys. 45, 111 (1973); H. Tawara and A. Russek, *ibid.* 45, 178 (1973); H. Tawara, Research Information Center Document IPPJ-AM-1, Nagoya University, Nagoya, Japan (unpublished).

[6]G. Basbas, W. Brandt, and R. Laubert, Phys. Rev. A 7, 983 (1973), and references contained therein.

[7]G. Basbas, W. Brandt, and R. Laubert, Phys. Rev. A 17, 1655 (1978).

[8]C. D. Lin, S. C. Soong, and L. N. Tunnell, Phys. Rev. A 17, 1646 (1978); C. D. Lin, *ibid.* 19, 1510 (1979); C. D. Lin and L. N. Tunnell, *ibid.* 22, 76 (1980).

[9]J. F. Reading and A. L. Ford, J. Phys. B 12, 1367 (1979); A. L. Ford, J. F. Reading, and R. L. Becker, *ibid.* 12, 2905 (1979); R. L. Becker, A. L. Ford, and J. F. Reading, *ibid.* 13, 4059 (1980).

[10]For a review see T. J. Gray, in *Methods of Experimental Physics, Volume 17,* edited by P. Richard (Academic, New York, 1980), Ch. 5, pp. 193—278.

[11]M. R. Khan, D. Crumpton, and P. E. François, J. Phys. B 9, 455 (1976).

[12]F. D. McDaniel, T. J. Gray, and R. K. Gardner, Phys. Rev. A 11, 1607 (1975).

[13]C. G. Soares, R. D. Lear, J. T. Sanders, and H. A. Van Rinsvelt, Phys. Rev. A 13, 953 (1976).

[14]F. D. McDaniel, T. J. Gray, R. K. Gardner, G. M. Light, J. L. Duggan, H. A. Van Rinsvelt, R. D. Lear, G. H. Pepper. J. W. Nelson, and A. L. Zander, Phys. Rev. A 12, 1271 (1975).

[15]G. Monigold, F. D. McDaniel, J. L. Duggan, R. Mehta, R. Rice, and P. D. Miller, in *Proceedings of the Fourth Conference on the Scientific and Industrial Applications of Small Accelerators, Denton, Texas,* edited by J. L. Duggan and I. L. Morgan (IEEE, New York, 1976), pp. 70—74.

[16]J. Hall, P. Richard, T. J. Gray, C. D. Lin, K. Jones, B. Johnson, and D. Gregory, Phys. Rev. A 24, 2416 (1981).

[17]J. Hall, P. Richard, T. J. Gray, K. Jones, B. Johnson, and D. Gregory, Phys. Lett. 90A, 129 (1982).

[18]A. Schmiedekamp, T. J. Gray, B. L. Doyle, and U. Schiebel, Phys. Rev. A 19, 2167 (1979).

[19]K. A. Jamison, C. W. Woods, R. L. Kauffman, and P. Richard, Phys. Rev. A 11, 505 (1975).

[20]F. P. Larkins, J. Phys. B 4, L29 (1971).

[21]J. Hall, Ph.D. dissertation, Kansas State University, 1981 (un-

published).
[22]For a review see F. Hopkins, in *Methods of Experimental Physics, Volume 17,* Ref. 10, Ch. 8, pp. 355—431.
[23]J. Newcomb, M. S. thesis, Kansas State University, 1979 (unpublished).
[24]R. L. Kauffman, J. H. McGuire, P. Richard, and C. F. Moore, Phys. Rev. A 8, 1233 (1973).
[25]K. W. Hill, B. L. Doyle, S. M. Shafroth, D. H. Madison, and R. D. Deslattes, Phys. Rev. A 13, 1334 (1976).
[26]H. Tawara, P. Richard, T. J. Gray, P. Pepmiller, J. R. Macdonald, and R. Dillingham, Phys. Rev. A 19, 2131 (1979).
[27]T. W. Tunnell and C. P. Bhalla, Phys. Rev. Lett. 86A, 13 (1981).
[28]G. Lapicki and F. D. McDaniel, Phys. Rev. A 22, 1896 (1980).
[29]See AIP document No. PAPS PLRAA-28-99-32 for 32 pages of experimental cross sections. Order by PAPS number and journal reference from American Institute of Physics, Physics Auxiliary Publication Service, 335 East 45th Street, New York, N.Y. 10017. The price is $1.50 for each microfiche or $5.00 for photocopies. Airmail additional. Make checks payable to the American Institute of Physics.
[30]R. Rice (private communication).
[31]C. W. Woods, R. L. Kauffman, K. A. Jamison, N. Stolterfoht, and P. Richard, Phys. Rev. A 12, 1393 (1975).
[32]W. Fritsch and C. D. Lin, J. Phys. B 15, 1255 (1982).